Vapour phase oxidation of cumene by molecular oxygen over MCM-41 supported cobalt oxide catalyst

S. Vetrivel and A. Pandurangan*

Department of Chemistry, Anna University, Chennai 600 025, India

Received 12 December 2003; accepted 26 March 2004

Si-MCM-41 and Al-MCM-41 supported cobalt oxide catalysts were prepared and characterized by XRD. The surface area, pore size and wall thickness was calculated by applying BET equation and BJH method using nitrogen sorption technique. DR UV-VIS confirm the presence of cobalt oxide as isolated particle in the framework positions of the MCM-41 mesostructure. The vapour phase oxidation of isopropyl benzene with CO_2-free air as the oxidant was studied over cobalt oxide supported unwashed and washed Si-MCM-41 and Al-MCM-41 catalyst. Isopropyl benzene conversion increased with increase in temperature from 200 to 300 °C, but at 325 °C it decreased. Formation of coke was noted at all the temperatures. Cumenehydroperoxide, 1,2-epoxyisopropylbenzene, acetophenone and styrene were the products observed in this reaction. Of the products cumenehydroperoxide was found to be more selective over all the catalysts. Both unwashed and washed catalysts were found to have nearly the same activity. Due to more dispersion, the active sites in the latter catalysts compensates its low cobalt oxide content in producing activity equal to the former catalysts. The study of time on stream indicated decrease in conversion due to coke formation.

KEY WORDS: MCM-41; oxidation; air; cumene; cumenehydroperoxide; cobalt oxide.

1. Introduction

The catalytic oxidation with dioxygen traditionally holds a very prominent place in the petrochemical industry, where it is by far the most important technology for the upgrading of hydrocarbons [1]. The dominant position of dioxygen as the oxidant for bulk chemical oxy-functionalizations is due to the fact that it is the only economically and environmentally feasible oxidant for large scale processing. The most widely used route for hydroperoxide production proceeds through the following steps. (a) alkylation of benzene with propylene to cumene, (b) vapour phase oxidation of cumene to cumenehydroperoxide and (c) cumenehydroperoxide cleavage to acetophnone and 1,2-epoxyisopropylbenzene [2]. Many researchers have worked previously for cumene oxidation reaction with Zircona-, titania-, and alumina-based complex oxides, salane Co II) and polymer-supported catalyst [3–5]. In spite of the excellent performance of these catalysts, there are some drawbacks. For instance, the catalysts undergo slow decomposition at a reaction temperature of 363 K, and hence speeding up of the reaction rate by employing these catalysts is impossible [5]. The main aim of this study is to use MCM-41 supported cobalt oxide catalysts, circumventing the above said drawbacks. As the support has mesopores, they are capable of holding metal oxides in nanodimentions with high catalytic activity. The catalyst precursor [6–9], the support [10–12], the preparation method [7–9,12–15] and the metal loading [6,10] are observed to influence the oxidation behavior of cobalt catalyst.

Therefore in the present study, cobalt oxide impregnated MCM-41 catalysts were synthesized and characterized. Their catalytic activity for the oxidation of cumene using air as an oxidant was examined. The effects of reaction temperature, weight hourly space velocity and time on stream on conversion and products selectivity were examined and the results discussed.

*To whom correspondence should be addressed.
E-mail: pandurangan_a@yahoo.com

2. Experimental

2.1. Liquid phase impregnation

The parent Si-MCM-41 and Al-MCM-41 were synthesized according to previous reports [16–18] using $C1_2H_{25}N(CH_3)_3Br$ as the template. Cobalt oxide impregnated samples were prepared by overnight stirring of 3 g of Si-MCM-41 or Al-MCM-41 in 50 mL; 0.3 M cobalt nitrate solutions. The material was filtered and gently washed in deionized water in order to remove any ions adsorbed on the external surface. The filtrate was then dried by evaporation under reduced pressure, and finally calcined in air at 823 K for 6 h.

2.2. Physico-chemical characterization

The aluminium content in Al-MCM-41 (Si/Al = 99 and 158) was determined using ICP-AES with allied analytical ICAP 9000. The Co content in Co-SiMCM-41 and Co-AlMCM-41 was estimated using AAS (GBC932 plus) by flowing acetylene and air at a rate of 1.85 and 13.1 L/min, respectively.

1011-372X/04/0600–0167/0 © 2004 Plenum Publishing Corporation

The crystalline phase identification and phase purity determination of the before and after impregnated samples of Si-MCM-41, Al-MCM-41 (99) and Al-MCM-41 (158) were, carried out by XRD (Siemens D500) using nickel-filtered CuK_α radiation ($\lambda = 1.542$ Å). Nitrogen adsorption–desorption isotherms were analysed using a Nova-1000 (QUANTACHROME, Version 5.01) sorptometer at liquid nitrogen temperature. Before analysis, calcined and hydrothermally treated samples were dried at 130 °C and evacuated overnight in flowing argon at a flow rate of 60 mL min^{-1}. Surface area, pore size and wall thickness was obtained from these isotherms using the conventional BET and BJH equations. IR spectra of the sample were recorded on a Bruler IFS 66v FT-IR spectrophotometer using KBr pellets. Thermogravimetric-differential thermal analysis (TG-DTA) was carried out in a Rheometric scientific (STA 15 H^+) thermo balance. Ten to fifteen milligrams of as-synthesized sample Si-MCM-41, Al-MCM-41 (99) and Al-MCM-41 (158) were loaded, and the airflow used was 50 mL min^{-1}. The heating rate was 20 °C min^{-1} and the final temperature was 1000 °C.

^{29}Si MAS-NMR spectra were recorded in a DRX-500 FT-NMR spectrometer at a frequency of 59.64 MHz, spinning speed of 8 kHz, pulse length of 2.50 μs (45° pulse), delay time of 10 s and spectral width of 335 ppm. Two thousand scans were acquired with reference to trimethylsilylpropanesulfonic acid (TSP). Solid-state ^{27}Al MAS-NMR spectra were recorded at a frequency of 104.22 MHz, spinning rate of 8 kHz, pulse length of 1.0 μs, delay time of 0.2 s and spectral width of 330 ppm. The total number of scans was 150 and the line broadening was 50 Hz. The ^{27}Al chemical shifts were reported in relation to the solution of aluminium nitrate. Diffuse reflectance (DR) spectra were recorded between 350 and 2000 nm on a Shimadzu UV-240 spectrometer in the UV–Vis region using $BaSO_4$ as a reference.

2.3. Catalytic activity studies

The reactor system was a fixed-bed, vertical type reactor made up of a quartz tube of 40 cm length and 2 cm internal diameter. The quartz reactor was heated to the requisite temperature with the help of a tubular furnace controlled by a digital temperature controller cum indicator. At the bottom of the reactor a piece of thermowool was placed, over which a chromel–alumel thermocouple was kept to measure the temperature at the middle of the catalyst bed with an accuracy of ±5 °C. About 0.3 g of the catalyst was placed in the middle of the reactor and supported on either side with a thin layer of quartz wool and ceramic beads. The liquid reactant was injected in to the reactor containing the catalyst bed by a microdisplacement pump at a WHSV of 3.3 mL h^{-1}, with air 90 mL h^{-1}. The bottom of the reactor was connected to a coiled condenser and a receiver. The liquid product collected for the first 15 min of each run, normally covering an hour, was discarded and only the products obtained after this period was analysed. This was done to ensure the attainment of a steady state for the reaction over the catalyst and also to obtain a steady temperature in the furnace. The liquid products were analysed by a Gas Chromatography (HP 5890 series II) using a flame ionization detector and 50 m × 0.2 mm PONA column (Supelco). All the catalysts were regenerated by burning away the coke deposit formed on them from the previous reaction by passing a stream of pure dry air at a temperature of 500 °C for 8 h. The same catalyst was used for the study of WHSV and time on stream.

3. Results and discussion

3.1. ICP-AES and AAS analysis

Table 1 gives the ICP values obtained for the resulting solids. It can be seen that the Si/Al molar ratio of the solid is almost same as that of the starting mixtures, in agreement with what is usually observed for such synthesis. The results of AAS analysis to determine the cobalt content of the materials are given in the same table.

3.2. XRD

The XRD patterns of the calcined Si-MCM-41, Al-MCM-41 (99), Al-MCM-41 (158) samples are given in figure 1a. The XRD patterns are almost flat in the 2θ range of 20–30, indicating that no significant amount of conventional amorphous silica is present in the products.

Table 1
Elemental analysis of Co and Al containing MCM-41 catalysts

Samples	Si/Al	ICP	AAS-cobalt content			
			Unwashed		Washed	
			Theoretical (ppm)	Experimental (ppm)	Theoretical (ppm)	Experimental (ppm)
Si-MCM-41	–	–	11.644	11.413	11.644	9.100
Al-MCM-41 (99)	100	99	11.644	10.304	11.644	8.831
Al-MCM-41 (158)	150	158	11.644	9.658	11.644	7.924

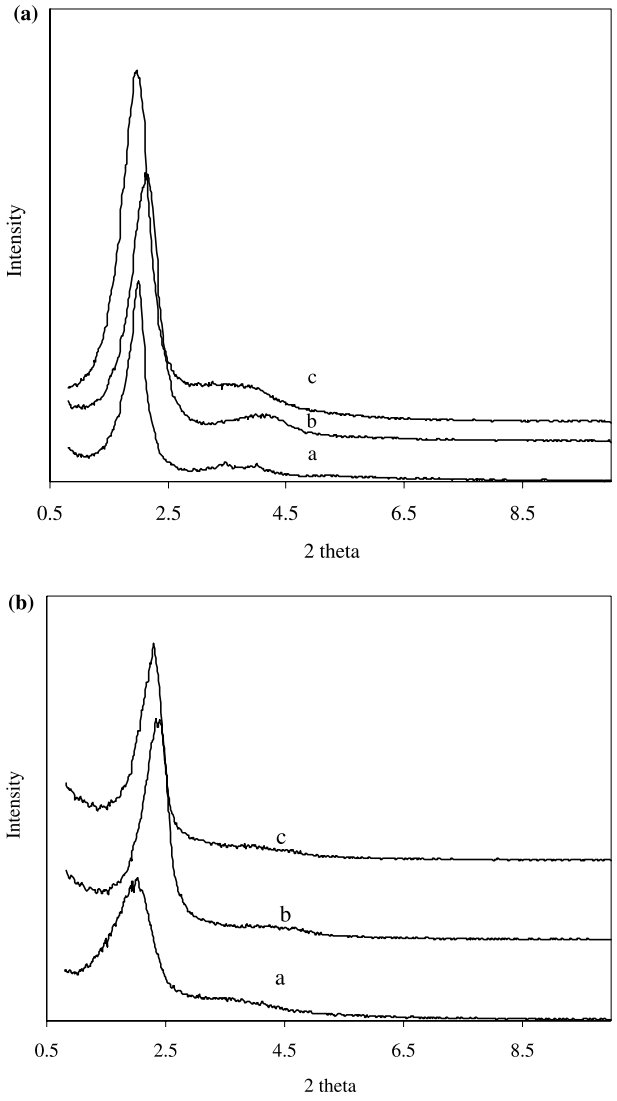

Figure 1a. XRD of (a) calcined Si-MCM-41, (b) Al-MCM-41 (99) and (c) Al-MCM-41 (158). Figure 1b. XRD of (a) calcined Co-MCM-41-U, (b) Co-A1MCM-41 (99)-U and (c) Co-A1MCM-41 (158)-U.

The pore-to-pore distance of Si-MCM-41, Al-MCM-41 (99) and Al-MCM-41 (158) with characteristic peaks of hexagonal symmetry at d_{100} was 43.68, 40.90 and 44.18 Å are given in table 2. Figure 1b presents the XRD patterns due to MCM-41 supported cobalt oxide catalysts. The intensity of the patterns due to 100 plane is decreased and that of 110 and 200 planes disappeared owing to radiation diffusion. It is due to the nanosize of impregnated particles present in the pores. The hexagonal unit cell parameter (a_0) was calculated using the following formula from $d_{100,}$ which was obtained from the peak in the XRD pattern by Bragg's equation ($2d \sin\theta = \lambda$, where $\lambda = 1.542$ Å for the CuK_α line). The value of a_0 was equal to the internal pore diameter plus one pore wall thickness.

3.3. Adsorption isotherm of nitrogen

Nitrogen adsorption isotherms of calcined Si-MCM-41, Al-MCM-41 (99) and Al-MCM-41 (158) measured at liquid nitrogen temperature (77 K). The results are presented in the Figure 2. Three well-defined stages may be identified: (1) a slow increase in nitrogen uptake at low relative pressure, corresponding to monolayer-multilayer adsorption on the pore walls; (2) a sharp step at intermediate relative pressures indicative of capillary condensation within mesopores; (3) a plateau with a slight inclination at high relative pressures associated with multilayer adsorption on the external surface of the crystals [19]. The isotherms suggest that Al incorporation results in a shift to lower pore size (pore-filling step at lower p/p_0) and that the decrease in pore size is greater at higher Al content. It is interesting to note from the isotherms that the presence of Al results in significant adsorption at high partial pressures (p/p_0). It is likely that the Al-MCM-41 samples are made up of inhomogeneous particles which give rise to interparticle voids. The data presented in table 2 indicate that the calcined Al-containing samples have thicker pore walls, larger distances between pore centers and larger BET areas than the siliceous MCM-41: The pore walls reported in this work are larger than those observed by Corma *et al.* [20].

3.4. FT-IR spectroscopy

Figure 3 shows the FT-IR spectra of as-synthesized and calcined Si-MCM-41, Al-MCM-41 (99) and Al-MCM-41 (158) materials. The as-synthesized samples exhibit adsorption bands around 2921 and 2851 cm^{-1} corresponding to C-H vibrations of the surfactant molecules. The broad bands around 3500 cm^{-1} may be attributed to surface silanols and adsorbed water

Table 2
Physicochemical characterization of calcined Si-MCM-41, Al-MCM-41 (99) and Al-MCM-41 (158)

Samples	Before impregnation		After impregnation		BET surface area ($m^2\ g^{-1}$)	Pore size (Å)	Wall thickness (Å)
	d_{100} (Å)	Unit cell–a_0 (Å)	d_{100} (Å)	Unit cell–a_o (Å)			
Si-MCM-41	43.68	50.44	42.89	49.53	998	27.6	33.2
Al-MCM-41 (99)	40.90	47.23	36.82	42.52	1036	31.5	13.6
Al-MCM-41 (158)	44.18	51.02	38.42	44.36	1102	30.8	16.0

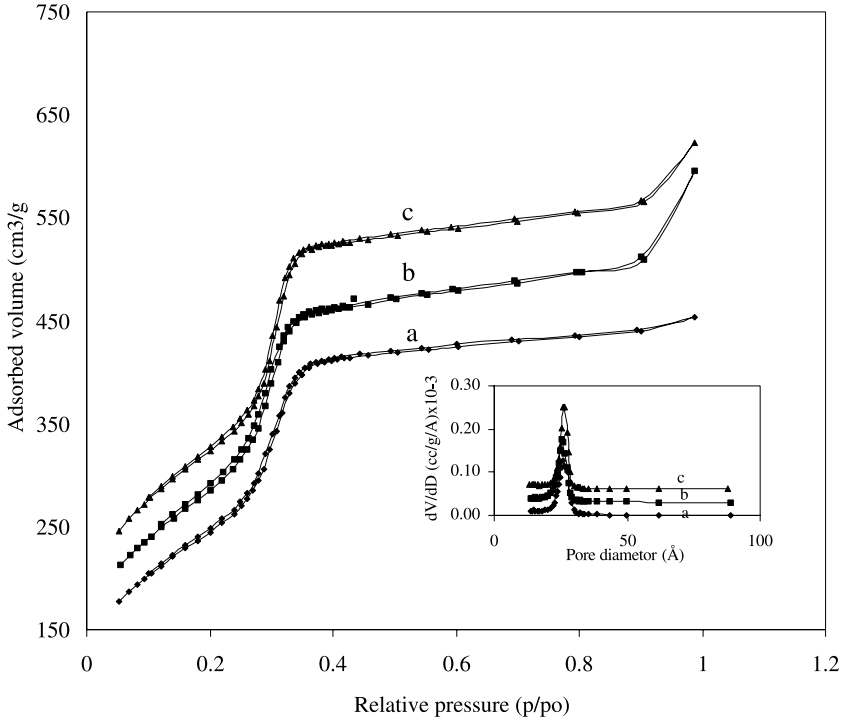

Figure 2. N_2 adsorption isotherm of (a) calcined Si-MCM-41, (b) Al-MCM-41 (99) and (c) Al-MCM-41 (158).

molecules, while deformational vibrations of adsorbed molecules cause the adsorption bands at 1623–1640 cm^{-1} [20]. The adsorption bands at 1057 and 1223 cm^{-1} are due to asymmetric stretching vibrations of Si–O–Si bridges. Based on less intense peaks at 2851 and 2921 cm^{-1} for the calcined samples, one could conclude that calcination completely eliminates the locked-in template. An adsorption band of 967 cm^{-1} assigned to a stretching vibration of Si–O–Al linkage was observed. As the aluminium content increased, an additional broad band around 3500 cm^{-1} was found.

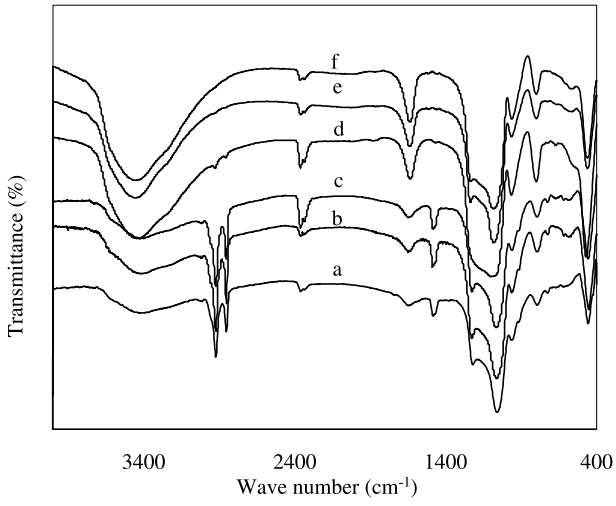

Figure 3. FT-IR spectra of (a) as-synthesized Si-MCM-41, (b) Al-MCM-41 (99) and (c) Al-MCM-41 (158) (d) calcined Si-MCM-41, (e) Al-MCM-41 (99) and (f) AlMCM-41 (158).

This was assigned to hydroxyl groups on octahedrally coordinated aluminium species [21].

3.5. TG-DTA

Thermogravimetric analyses of the samples show distinct weight losses that depend on framework composition (table 3). Three distinct steps can be distinguished: at 50–150, 150–350 and above 350 °C. The weight loss due to the desorption of water was observed between 50 and 150 °C. The weight loss at the stage of 150–350 °C can be ascribed to the decomposition of the organic species. The weight loss above 350 °C can be assigned to coke calcination and the loss of silanol groups. The total weight loss at 1000 °C for Si-MCM-41, Al-MCM-41 (99) and Al-MCM-41 (158) samples are in the 51.36%, 51.05% and 52.57%, respectively, without any clear dependence on the Si/Al ratio or aluminium source of the sample.(see figure 4) However, the distribution of successive weight losses depends on the framework Si/Al ratio [22,23]. Thus, weight loss was

Table 3
Thermogravimetric results (in air) for the MCM-41 type materials

Samples	Weight loss (wt%)			
	Total	50–150 °C	150–350 °C	350–550 °C
Si-MCM-41	52.36	11.43	32.49	8.44
Al-MCM-41 (99)	51.05	11.52	27.60	11.93
Al-MCM-41 (158)	52.57	11.61	9.47	11.47

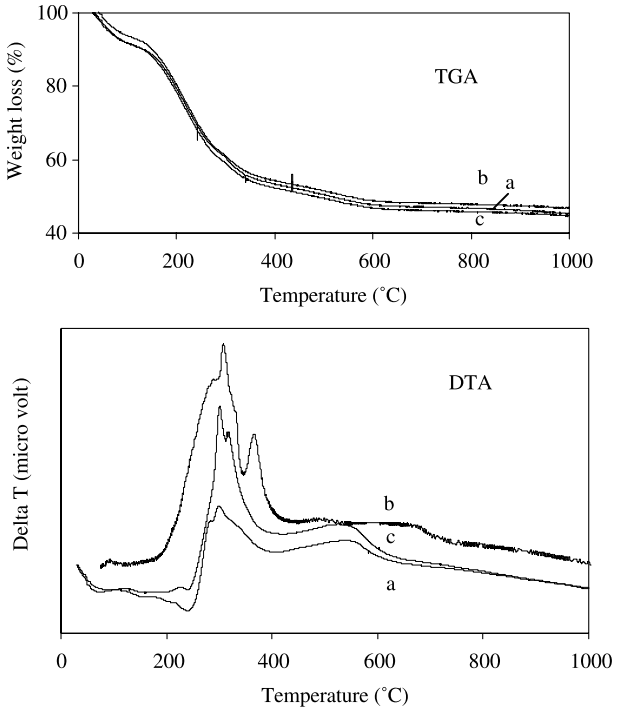

Figure 4. TGA curve of (a) as-synthesized Si-MCM-41, (b) Al-MCM-41 (99) and (c) Al-MCM-41 (158).

higher in the Al-MCM-41 (158) than that in the other two, where the Al content was less than in the others.

3.6. ^{29}Si and ^{27}Al MAS-NMR

The ^{29}Si MAS-NMR spectra of purely siliceous MCM-41 show (figure 5) a signal centered at −110.9 ppm attributed to Q^4, environments and a shoulder at −104 ppm for Q^3, $Si(OSi)_3$ OH sites. These spectral features coincide well with those reported by the previous workers [24,25]. In ^{27}Al MAS-NMR spectra of the samples, the peak around 53.7 ppm for Al-MCM-41 (99) and 52.1 ppm for Al-MCM-41 (158) are attributed to the presence of aluminium in tetrahedral coordination [24–26]. ^{27}Al MAS-NMR of the calcined Al-MCM-41 (99 and 158) shows a less intense peak at −0.37 ppm. This peak is due to extra framework aluminium species in octahedral coordination and it is expected to arise out of the framework dealuminium during calcination [26].

3.7. DR UV–Vis spectroscopy

The coordination environment of cobalt in unwashed Co-MCM-41 and Co-Al-MCM-41 (99) was analysed by DRS, and DR spectra of calcined samples are shown in figure 6. An intense band centered at ca.520 nm is

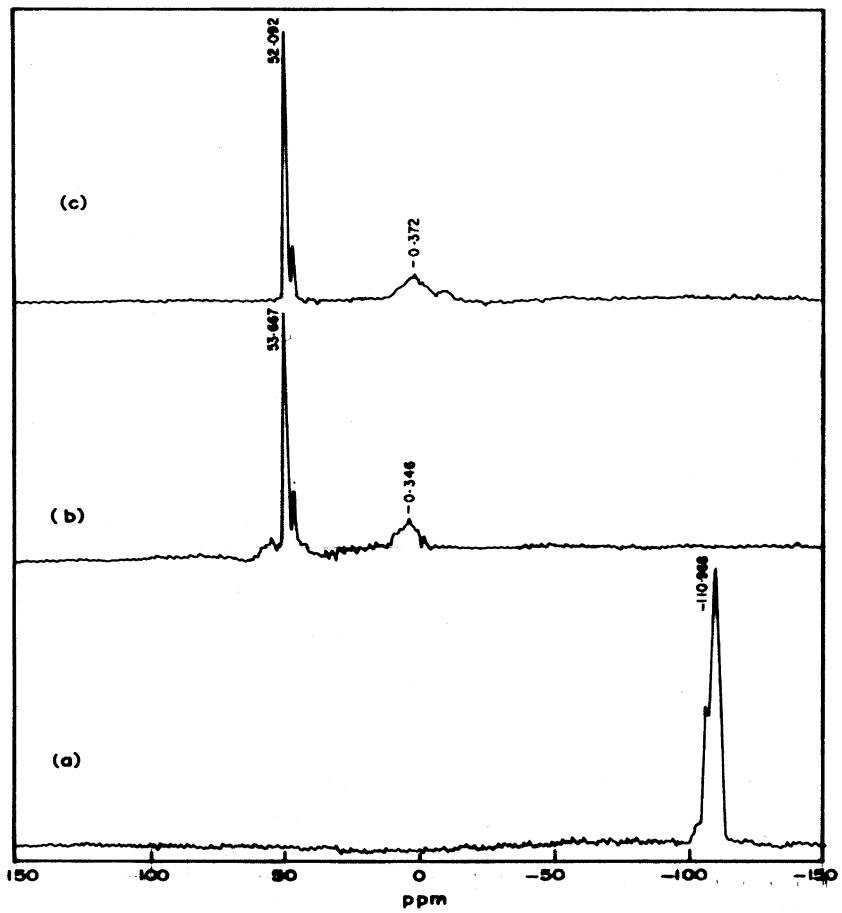

Figure 5. ^{29}Si MAS NMR and ^{27}Al MAS NMR spectra of (a) Si-MCM-41, (b) Al-MCM-41 (99) and (c) Al-MCM-41 (158).

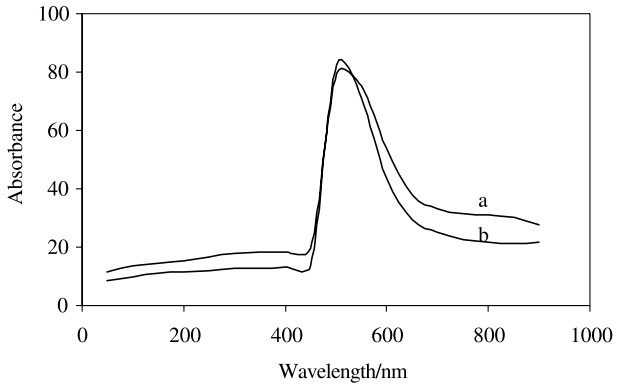

Figure 6. DR UV–Vis spectra of (a) calcined Co-MCM-41-U, (b) Co-AlMCM-41 (99)-U and (c) Co-AlMCM-41 (158)-U.

observed, implying the presence of a ligand-to-metal charge transfer involving isolated transition metal sites [27]. From the DR UV spectrum one can learn that, for the lilac Co (NO_3)–SiO_2, ca.520 nm, the cobalt oxide is incorporated into the silicate with an octahedral co-ordination sphere is observed.

3.8. Influence of temperature

The vapour phase oxidation of isopropylbenzene over cobalt oxide impregnated unwashed (U) catalysts, Co-MCM-41, Co-AlMCM-41 (99) and Co-AlMCM-41 (158), at 200, 225, 250, 275, 300 and 325 °C was studied with CO_2-free air as the oxidant. The results of isopropylbenzene conversion and selectivity to cumenehydroperoxide (CHP), 1,2-epoxyisopropyl benzene

Table 4
Oxidation of cumene: variation with temperature

Catalysts	Temperature (°C)	Conversion (wt%)	Product selectivity (%)				
			CHP	1,2-EIPB	AP	Styrene	Others
Co-MCM-41-U	200	32.8	45.7	30.5	19.1	4.7	0
	225	38.1	47.2	21.6	17.7	7.0	6.5
	250	43.2	56.4	16.8	14.9	8.5	3.4
	275	46.9	63.8	9.3	9.4	9.2	8.3
	300	50.1	81.3	3.7	5.1	9.9	0
	325	48.4	65.9	3.1	4.1	15.6	11.3
Co-AlMCM-41 (99)-U	200	31.0	39.8	29.0	21.8	5.9	3.5
	225	34.1	41.6	22.1	19.5	8.1	8.7
	250	36.7	47.4	18.7	15.2	12.4	6.3
	275	39.5	53.5	9.3	9.4	16.7	11.1
	300	45.5	64.7	4.1	5.8	17.1	8.3
	325	41.9	58.1	3.2	5.0	20.6	13.1
Co-AlMCM-41 (158)-U	200	29.9	33.1	28.5	24.8	6.1	7.5
	225	34.1	38.7	22.2	21.2	12.8	5.1
	250	36.8	40.3	16.9	19.5	14.4	8.9
	275	38.6	47.6	8.4	14.9	19.0	10.1
	300	43.8	57.0	5.5	8.1	20.1	9.3
	325	40.3	50.6	4.2	7.7	23.9	13.6
Co-MCM-41-W	200	30.1	44.4	31.2	19.3	4.3	0.8
	225	34.7	46.7	23.1	18.1	6.5	5.6
	250	37.0	53.1	17.0	14.9	9.0	6.0
	275	40.5	67.1	9.6	8.9	10.5	3.9
	300	46.5	71.4	5.1	4.2	12.0	7.3
	325	42.2	68.9	4.2	3.6	15.6	10.7
Co-AlMCM-41 (99)-W	200	28.0	33.3	27.0	22.3	5.5	11.9
	225	32.8	39.6	22.1	19.8	8.1	10.4
	250	35.0	47.5	19.3	17.0	12.0	4.2
	275	38.0	56.0	11.8	9.6	16.3	6.3
	300	43.4	63.3	8.0	5.8	18.0	4.9
	325	40.7	58.1	5.2	4.7	21.7	10.3
Co-AlMCM-41 (58)-W	200	28.1	33.1	29.0	26.0	7.0	4.9
	225	32.0	37.7	24.3	22.5	11.8	3.7
	250	34.1	40.3	16.7	19.8	15.5	7.7
	275	38.6	48.5	10.5	14.9	19.1	7.0
	300	42.0	55.1	7.1	10.4	22.2	5.2
	325	39.0	52.4	4.3	8.4	25.0	9.9

Reaction condition: 0.3 g of catalyst; flow rates: 1 mL/h for reactants and 90 mL/h for air.

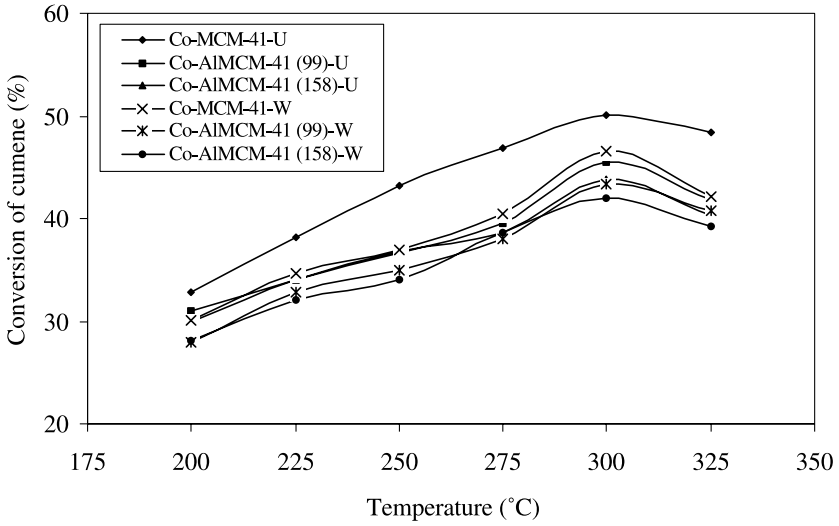

Figure 7. Effect of temperature on the conversion of cumene over Co-MCM-41-U, Co-AlMCM-41 (99)-U, Co-AlMCM-41 (158)-U, Co-MCM-41-W, Co-AlMCM-41(99)-W and Co-AlMCM-41 (158)-W.

(1,2-EIPB), acetophenone (AP) and styrene are presented in table 4. Co^{3+} catalyses oxidation of cumene by abstracting the tertiary hydrogen as shown in the following reaction scheme. This mechanism was also reported in the literature [28]. The cumene radical reacts with molecular oxygen to produce alkyl peroxide. The peroxide in turn abstracts hydrogen from cumene to form isopropylhydroperoxide. The arolkylhydroperoxide is decomposed catalytically to yield acetophenone and 1,2-EIPB.

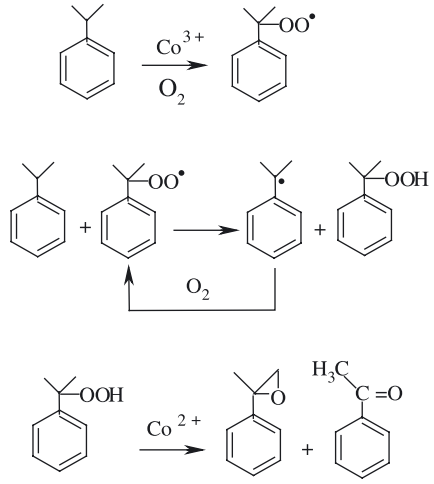

Conversion increases from 200 to 300 °C, but at 325 °C it shows a slight decrease (figure 7). As coke formation is observed at all temperatures, and it is to be more favoured with increase in temperature, the increase in conversion between 200 and 300 °C is not high. Nearly similar values of conversion at each temperature over all the catalysts suggest similar level of dispersion of cobalt oxide on the catalyst surface. It is once again supported by nearly similar level of impregnation of cobalt oxide as evidenced from AAS analysis (table 1). In order to test whether the carbon deposits or sintering of metal oxide is important for catalyst deactivation, the spent catalyst, Co-MCM-41-U was again tested for activity under identical conditions after activation. Before activation conversion of cumene was 50.1% and the same used catalyst after activation gave 49.2% conversions, proving thus only carbon deposit as the cause for catalyst deactivation.

Among the products CHP was found to be formed with more selectivity than the others at all the temperatures studied. Its selectivity increases from 200 to 300 °C, but at 325 °C it decreases (figure 8). The decomposition of CHP may not be entirely free, but to be assisted by the catalyst, since the selectivity is not increased at 325 °C. Similar to conversion, CHP selectivity shows similar trend of increase with increase in temperature over all the catalysts up to 300 °C.

The selectivity to 1,2-EIPB and acetophenone decreases with increase in temperature. The selectivity of 1,2-EIPB is more than acetophenone at lower temperatures, but at higher temperature the trend is reversed. But the increase in selectivity of acetophenone is not very much compared to 1,2-EIPB. This change is clearly evident for all the catalysts from the data in the table 4.

The increase in the selectivity of CHP with increase in temperature, and the decrease in the selectivity of 1,2-EIPB and acetophenone with increase in temperature suggest the latter product might be obtained from the decomposition of CHP. The formation of these two products also reveals the decomposition of CHP is to be assisted by the catalyst. At higher temperature the decomposition of CHP is not favoured due to less adsorption of it on the catalyst surface. The less selectivity of CHP at 325 °C contradicts this view, as

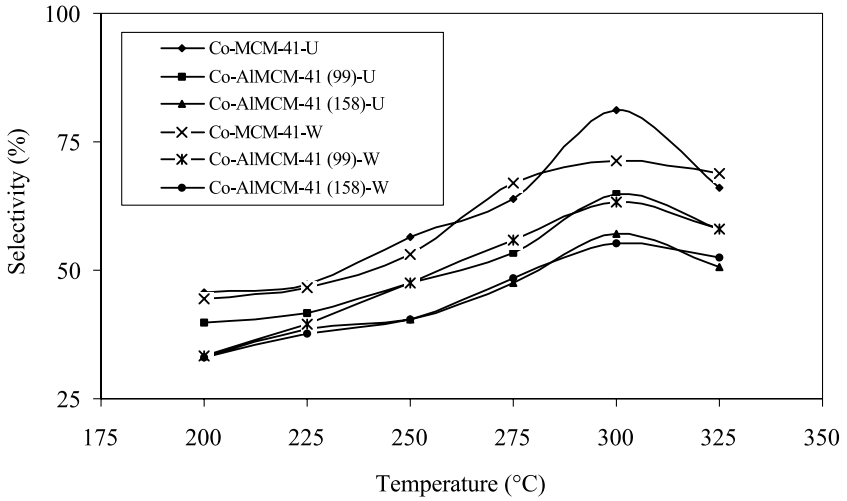

Figure 8. Effect of temperature on the product selectivity of CHP over Co-MCM-41-U,Co-AlMCM-41 (99)-U, Co-AlMCM-41 (158)-U, Co-MCM-41-W, Co-AlMCM-41 (99)-W and Co-AlMCM-41 (158)-W.

the expected value is to be high. The less value may be due to formation of styrene with more selectivity directly from cumene via radical mechanism as shown in the following reaction scheme:

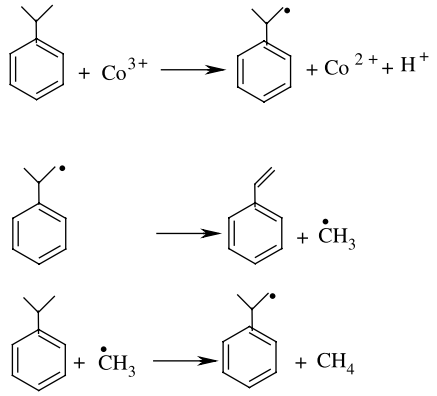

Co^{3+} at high temperature is expected to abstract electron from the methyl group of cumene. The arolkyl radical decomposes to produce styrene. The Co^{2+} formed in this reaction will catalyse arolkylhydroperoxide as given in the previous mechanism. Formation of styrene directly from cumene was also established by passing the latter over the catalyst in the absence of air. Styrene was obtained with 7.8% yield at 300 °C. The same trends of selectivity for all the products over all the catalysts suggest occurring of similar mechanism for different reaction in this oxidation process. As the conversion over all the catalysts nearly remains the same, the protonic sites of the catalyst of Co-AlMCM-41 (99) and Co-AlMCM-41 (158) may not have any influence in this reaction.

The reaction results obtained over surface washed (W) cobalt oxide impregnated catalysts are shown in the table 4. Cumene conversion exhibits a similar trend of increase with increase in temperature from 200 to 300 °C, and decrease at 325 °C for all the catalysts. The results of conversion are illustrated in figure 7. But comparison of conversion over these catalysts with the unwashed catalysts shows nearly similar values (there is a decrease in conversion but the decrease is not much). Hence, during washing, the metal nitrates may not be much expelled, which would be possible only if cobalt nitrate is largely present inside the channel. Hence the reaction might be expected to occur largely within the pores.

The selectivity to CHP also exhibits similar trend of increase with increase in temperature up to 300 °C and decrease at 325 °C as that of the previous set of the catalysts (figure 8). Similarly, the selectivity patterns of 1,2-EIPB, acetophenone and styrene are also retained in this catalysts as the previous ones in the temperature range studied. It might be stated that very high-level dispersion of metal oxides in this catalyst after washing might be the cause of maintaining of nearly similar conversion and product selectivity as that of the previous catalysts. It could be expected more particle size for previous catalysts due to more loading than the present set of catalysts. Different amount of cobalt oxide content for both group of catalysts (unwashed and washed) is also evidence from the AAS studies.

The reaction was also studied over freshly silica [29] supported cobalt oxide (0.3 M loading). When cumene was passed over this catalyst, to our surprise, at 250, 275 300 and 325 °C, the conversions were found to be 4.8%, 9.2%, 16.4% and 11.3% which are very low compared to MCM-41 supported cobalt oxide catalyst. We feel, it might be due to large size of the metallic oxide.

3.9. *Influence of cumene content in the feed*

The effect of cumene content in the feed on conversion and products selectivity over the unwashed catalysts was studied at 300 °C. The reaction results are

Table 5
Oxidation of cumene: variation with WHSV

Catalysts	WHSV (h^{-1})	Conversion (wt%)	Product selectivity (%)				
			CHP	1,2-EIPB	AP	Styrene	Others
Co-MCM-41-U	3.3	50.1	81.3	3.7	5.7	8.7	1.2
	6.7	46.5	67.3	9.8	7.9	5.6	9.4
	10.0	41.2	60.1	16.7	8.1	3.5	11.6
	13.3	37.8	57.1	28.9	10.3	2.9	0.8
Co-AlMCM-41 (99)-U	3.3	45.5	64.7	4.1	5.8	17.1	8.3
	6.7	40.3	54.2	11.6	8.8	13.5	11.9
	10.0	37.7	47.5	19.1	10.6	11.3	11.5
	13.3	34.9	44.3	26.6	13.1	8.6	7.4
Co-AlMCM-41 (158)-U	3.3	43.8	57.0	5.5	8.1	20.1	9.0
	6.7	41.5	53.1	10.0	11.1	15.2	10.6
	10.0	35.8	45.3	18.6	13.3	12.8	10.0
	13.3	34.7	44.0	27.7	16.0	9.0	3.3
Co-MCM-41-W	3.3	45.5	71.4	5.1	4.2	12.0	7.3
	6.7	42.2	64.8	12.5	9.0	10.5	3.2
	10.0	39.8	61.4	19.4	10.1	8.8	0.3
	13.3	36.8	56.1	25.0	11.8	5.7	1.4
Co-AlMCM-41 (99)-W	3.3	43.4	63.6	8.0	5.8	18.0	4.9
	6.7	39.9	57.1	12.0	9.0	15.1	6.8
	10.0	37.5	52.0	17.6	9.5	11.3	9.6
	13.3	35.0	40.3	24.4	15.0	9.1	11.2
Co-AlMCM-41 (58)-W	3.3	42.0	55.1	7.1	10.4	22.2	5.2
	6.7	40.3	51.1	11.2	12.5	17.5	7.7
	10.0	38.4	47.0	16.9	13.0	14.9	8.2
	13.3	35.8	44.3	23.8	15.8	11.8	4.3

Reaction condition: 0.3 g of catalyst, temperature 300 °C, and flow rate of air 90 mL/h.

presented in the table 5. Conversion decreased with increase in the cumene content over all the catalysts. Since the flow rate of air was kept at 90 mL/h, nearly the same contact time for cumene over the active sites of the catalyst irrespective of its content in the feed is expected. The conversion decreased; hence this decrease in conversion might be due to increase in the formation of molecular clusters of cumene with increase in its content in the feed. These molecular clusters prevent chemisorption and subsequent decomposition of cumene over the active sites.

The selectivity of CHP decreased with increase in the cumene content in the feed over all the catalysts. The high selectivity at lower content of cumene is attributed to decrease in the amount of Co(III) sites to chemisorption and subsequent decomposion of CHP. The less amount of Co(III) is due more conversion of it to Co(II) due to more formation of isopropylphenyl free radical. The decrease in the selectivity with increase in the content of cumene in the feed very well substantiates more and more formation of molecular clusters with increase in the cumene content. As there is less adsorption of cumene there would be more availability of Co(III) states inorder to chemisorb, decompose and reduce the selectivity of CHP. The increase in the selectivity of 1,2-EIPB and acetophenone also conforms the above suggestion for formation of molecular clusters at high cumene content. Formation of styrene with more selectivity at lower cumene content in the feed and less selectivity at higher content in the feed also provides support for the increased formation of molecular clusters with increase in the cumene content.

The effect of cumene content in the feed on conversion and product selectivity was examined over washed catalysts. The results are presented in the table 5. The conversion decreased with increase in the cumene content over all the catalysts. This trend is similar to the previous set of catalysts as discussed in the previous sections. The conversion is nearly same as that of the unwashed catalyst. The selectivity to CHP decreases with increase in the cumene content in the feed over all the catalyst similar to the previous set of catalyst.

The increase in the selectivity of 1,2-EIPB and acetophenone, and decrease in the selectivity of styrene over all the catalyst would also be accounted based on the formation of molecular clusters as discussed before.

3.10. Influence of time on stream

The effect of time on stream was studied at 300 °C over Co-MCM-41-U and Co-AlMCM-41 (99)-U. The

Table 6
Oxidation of cumene: variation with time on stream over unwashed Co-MCM-41 and Co-AlMCM-41 (99)

Catalysts	TOS (h)	Conversion (wt%)	Product selectivity (%)				
			CHP	1,2-EIPB	AP	Styrene	Others
Co-MCM-41	1	50.1	81.3	3.7	5.1	9.9	0
	2	48.0	83.1	4.3	3.8	7.8	1.0
	3	45.6	85.6	5.4	2.5	6.0	0.5
	4	42.1	87.9	6.0	2.0	4.1	0
	5	39.5	88.3	7.4	1.8	2.1	0.4
Co-AlMCM-41 (99)	1	45.5	64.7	4.1	5.8	17.1	8.3
	2	42.4	66.4	5.6	4.7	14.6	8.7
	3	40.1	71.6	7.0	3.0	13.0	5.4
	4	38.9	74.6	8.2	2.8	10.8	3.6
	5	37.2	77.0	9.0	1.7	10.0	2.3

Reaction condition: 0.3 g of catalyst, flow rates: 1 mL/h for reactants, temperature 300 °C, and flow rate of air 90 mL/h.

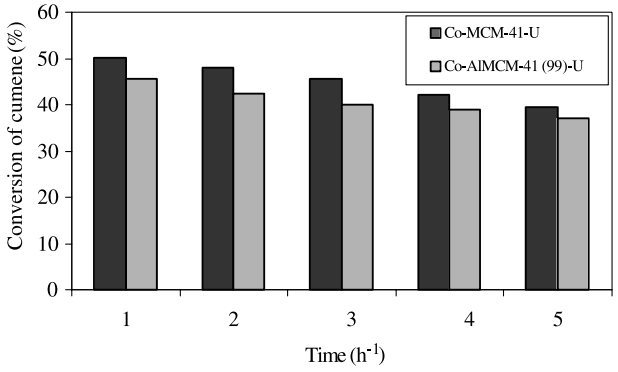

Figure 9. Effect of time on stream on the conversion of cumene over unwashed Co-MCM-41 and Co-AlMCM-41 (99).

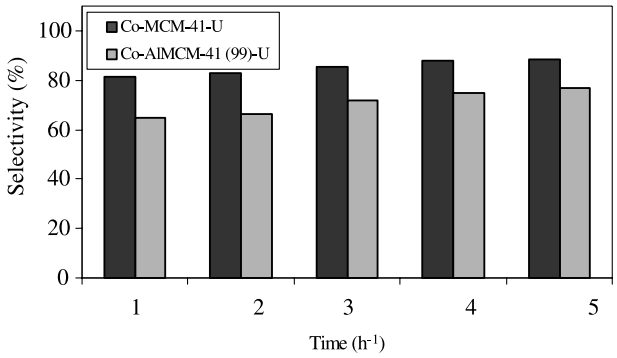

Figure 10. Effect of time on stream the product selectivity of CHP over unwashed Co-MCM-41 and Co-AlMCM-41 (99).

flow rate of cumene was 1 mL/h and air was 90 mL/h. The study was carried out for 5 h of stream, and the results are presented in the table 6. Conversion decreased with increase in stream over both the catalysts due to coke formation. The results of conversion are illustrated in figure 9. The selectivity to CHP increased with increase in stream (figure 10) due to blocking of active sites that assists its decomposition to 1,2-EIPB and acetophenone. Though the selectivity of 1,2-EIPB and acetophenone follows same trend in the earlier study, here the selectivity to 1,2-EIPB increases with increase in stream and to acetophenone decreases with increase in stream. This observation suggests existence of acid sites of different strengths.

Though both the products are formed by the decomposition of CHP, formation of acetophenone might be requiring acid sites of more strength than 1,2-EIPB, as the more active sites would be rapidly blocked by coke. The selectivity to acetophenone decreased with increase in stream. Since the formation 1,2-EIPB requires weak acid sites, its selectivity increased with increase in stream, as these sites are not blocked by coke. As the strong acid sites are more and more blocked with increase in stream, there would be more transport of CHP to weak acid sites to yield 1,2-EIPB with more selectivity. The selectivity to styrene decreased with increase in stream over both the catalysts due to coke formation. This decrease of selectivity also suggests requiring of more active sites for its formation.

4. Conclusion

Cobalt oxide impregnated Si-MCM-41 and Al-MCM-41 catalyst are found to be active for vapour phase oxidation of cumene to yield CHD 1,2-epoxyispropylbenzene, acetophenone and styrene. Significant conversion is obtained from 200 to 300 °C. Coke formation is noted at all the temperatures. One important observation in the study is the formation and the high selectivity of CHP. High conversion, and selectivity to CHP was retained even for 5 h stream. Both surface unwashed and washed catalysts give similar conversion and products selectivity. Presences of protonic sites in the Al-MCM-41 do not seem to be harmful in the study. Harmless air is used as an oxidant as a substitute for H_2O_2.

References

[1] R.W. Fisher,and F.Rohrschied, in: *Applied Homogeneous Catalysis with organometallic Compunds*, Vol.1, eds. B.Cornils and W.A. Herrmann (VCH, Weinheim, 1996).

[2] P. Andrigo, A. Caimi, P. Cavalieri d'Oro, A. Fait, L. Roberti, M. Tampieri and V.Tartari, Ind. Eng. Sci. 47(9–11) (1992) 2511.

[3] Y.V. Maksimov, I.P. Suzdalev, M.V. Tsodikov, V.Y. Kugel, O.V. Bukhtenko, E.V. Slivinsky and J.A. Navio, J. Mol. Catal. A: Chem. 105 (1996) 167.

[4] Y.F. Hsu, M.H. Yen and C.P. Cheng, J. Mol. Catal. 105 (1996) 137.

[5] Y.F. Hsu and C.P. Cheng, J. Mol. Catal. A: Gen. 120 (1997) 109.

[6] M.P. Rosynek and C.A. Polanky, Appl. Catal. 73 (1991) 97.

[7] E. van Steen, G.S. Sewell, R.A. Makhothe, C. Micklethwaite, H. Manstein, M. De Lange and C.T. O'Connor, J. Catal. 162 (1996) 220.

[8] L.B. Backman, A. Rautiainen, A.O.I. Krause and M. Lindblad, Catal. Today 43 (1998) 11.

[9] Y. Okamoto K. Nagata, T. Adachi, T. Imanaka, K. Inamura and T. Takyu, J. Phys. Chem. 95 (1991) 310.

[10] G.S. Sewell, E. van Steen and C.T.O'Connor, Catal. Lett. 37 (1996) 225.

[11] S. Bessel, Appl. Catal. A: Gen. 96 (1993) 253.

[12] R.C. Reuel and C.H. Bartholomew, J. Catal. 85 (1984) 63.

[13] K.E. Coulter and A.G. Sault, J. Catal. 154 (1995) 56.

[14] R. Srinivasan, R.J. de Angelish, P.J. Reucroft, A.G. Dhere and J. Bentley, J. Catal. 116 (1989) 144.

[15] H. Ming and B.G. Baker, Appl. Catal. A: Gen. 123 (1995) 23.

[16] T. Abe, Y. Tachibana, T. Vematsu and M. Iwamoto. J. Chem. Soc. Chem. Commun. (1995) 1617.

[17] J.S. Beck, J.C. Vartuli, W.J. Roth, M.E. Leonowicz, C.J. Kresge, K.D. Schmitt, C.T.W. Chu, D.H. Olson, E.W. Sheppard, S.B. McCullen, J.B. Higgins and J.L. Schlinker, J. Am. Chem. Soc. 114 (1992) 10834.

[18] C.T. Kresge, M.E. Leonowicz, W.T. Roth, J.C. Vartuli and J.S. Beck, Nature 359 (1992) 710.

[19] S.J. Gregand and K.S.W. Sing, *Adsorption, Surface Area And Porosity*, 2nd ed. (Academic Press, New York, 1982).

[20] A. Corma, Chem. Rev. 97 (1997)2373.

[21] A.V. Kiseler and V.I. Lygin, *Infrared Spectrum of Surface Compounds and Adsorbed Substances* (Nauka, Moscow, 1992) (in Russian).

[22] A. Jentys, N.H. Phan and H. Vinek, J. Chem. Soc., Faraday Trans. 93 (1996) 3287.

[23] M. Busio, J. Janchen and J.H.C. Van Hooff, Micro. Mater 5 (1995) 211.

[24] A. Corma, Micro. Meso. Mater 4 (1997)249.

[25] S. Biz and M.L. Occelli, Catal. Rev. Sci. Eng. 40(3) (1998) 329.

[26] A. Matsumoto, H. Chen, K. Tsutsumi, M. Grun and K. Unger, Micro. Meso. Matter 32 (1999) 55.

[27] C.Y. Chen, H.X. Li and M.E. Davis, Micro. Mater 2 (1993) 17.

[28] Herman Pines, *The Chemistry of Catalytic Hydrocarbon Conversions* (Academic Press, London, 1981) and pp. 241.

[29] G. De, B. Karmakar and D. Ganfuli, J. Mater. Chem. 10 (2000) 2289.